Anomalous thermal properties of the Heusler alloy $Ni_{2+x}Mn_{1-x}Ga$ near the martensitic transition

Y. K. Kuo, K. M. Sivakumar, and H. C. Chen
Department of Physics, National Dong Hwa University, Hualien 97401, Taiwan

J. H. Su and C. S. Lue
Department of Physics, National Cheng Kung University, Tainan 70101, Taiwan
(Received 3 December 2004; revised manuscript received 11 April 2005; published 10 August 2005)

We present the measurements of electrical resistivity (ρ), specific heat (C_P), Seebeck coefficient (S), as well as thermal conductivity (κ) of the Heusler compounds $Ni_{2+x}Mn_{1-x}Ga$ from 10 to 400 K. A series of $Ni_{2+x}Mn_{1-x}Ga$ alloys were prepared with $x=0$, 0.04, 0.06, 0.10, 0.14, 0.18, and 0.24 to systematically study the effect of substitution on the martensitic and ferromagnetic transitions. Unusual sharp peaks were observed in both S and κ around the martensitic transition temperature (T_M), while a noticeable change of slope was seen in S and κ at the ferromagnetic transition temperature (T_C) in $Ni_{2+x}Mn_{1-x}Ga$ with $x<0.14$. For $x\geqslant 0.14$ the structural and magnetic phase transitions were found to merge together, as noticed from the sharp changes in all measured physical quantities. Existence of premartensitic transition (T_P) was unambiguously resolved in the stoichiometric compound Ni_2MnGa by the C_P measurement, although such a feature becomes less pronounced with increasing x and completely disappears for the compositions $x\geqslant 0.10$. Significant thermal hysteresis loops between heating and cooling cycles appear in the vicinity of T_M, which is associated with the presence of 7-layer and 5-layer modulated structures. In addition, huge peaks were observed in the thermal conductivity near T_M. We connected this observation to the nesting of the Fermi-level density of states, which is appropriate for the Peierls transition.

DOI: 10.1103/PhysRevB.72.054116 PACS number(s): 81.30.Kf, 72.15.Eb, 72.15.Jf, 75.50.Cc

I. INTRODUCTION

Cubic Heusler alloys with general formula X_2YZ, where X and Y are the transition metals and Z often is an element with sp-type valence electrons from columns III through VI in the Periodic Table, have been of considerable interest due to their unusual magnetic and transport properties.[1–8] Particularly, the Mn containing Heusler compound Ni_2MnGa is a ferromagnetic material with a displacive and diffusionless martensitic transition from high symmetry cubic structure (austenitic phase) to low symmetry tetragonal/ortorhombic structure (martensite phase) upon cooling to around 220 K.[3] Another appealing aspect of Ni_2MnGa is the existence of martensitic transition in this material which shows thermoplastic and reversible characteristics leading to the shape memory effect. Such a shape memory effect has attracted considerable attention towards application as actuation devices and smart materials. Neutron diffraction studies revealed that the martensitic transition in Ni_2MnGa could be described as a simple contraction along the $\langle 100\rangle$ direction of the cubic cell,[3] without any change in the atomic position (diffusionless). In spite of the sizeable displacement of atoms, the change in the unit cell volume is only 1%.

In recent years, compositional dependence on the structural and transport properties in these enthralling materials has been of considerable interest.[1–14] For the stoichiometric Ni_2MnGa, the martensitic transition temperature ($T_M \sim 220$ K) is well below the Curie temperature ($T_C \sim 380$ K). It was found that both T_M and T_C are very sensitive to the composition, and substitution of Ni in place of Mn decreases T_C but enhances T_M in $Ni_{2+x}Mn_{1-x}Ga$.[2,12,15] It was argued that a reduction of Mn content in Ni_2MnGa increases the spatial distance between Mn atoms, leading to a decrease in the exchange integral and hence the Curie temperature.[15] The structural phase transition is presumably driven by the band Jahn-Teller effect,[16] and is accompanied by a reduction in the unit-cell volume. The enhancement of T_M with respect to Ni substitution for Mn in Ni_2MnGa can be understood in terms of the increase of e/a ratio (electron concentration), which is known to increase the electronic energy of the system and consequently the T_M.[17,18] The compositional dependence of T_M and T_C in $Ni_{2+x}Mn_{1-x}Ga$ alloys have opened up the possibility of coupling the structural and magnetic transitions near 320 K for the compositions with the critical value of x_C between 0.18–0.20.[2,12,15] The perplexing part of this class of alloys is the anomalies observed around the martensitic transition region.[19,20] The incomplete condensation TA_2 phonon branch around 260 K (which is well above the $T_M \sim 220$ K) observed in the inelastic neutron scattering experiments and other investigations have uncovered the presence of a weakly first order intermediate/premartensitic transition (T_P).[2,8,11,21–29] It was proposed that the premartensitic transition is tip-off of the beginning of the martensitic transition and temperature at which ($\sim$260 K) the premartensitic transition occurs is composition independent and appears only for the samples with $T_M < \sim 270$ K.[2,28] As T_M increases beyond this critical value ($\sim$270 K), the premartensitic transition slowly diminishes as it overlaps with T_M. In addition to the premartensitic transition, an intermediate phase was also reported just below T_M for $Ni_{2.16}Mn_{0.84}Ga$, revealed by electrical resistivity measurements.[6] Further, it is still not clear about the nature of the structural phase transition, whether it is athermal or isothermal.[24,30–34] On this basis, intense investigations are being carried out recently in order to explore the

very complex characteristics of the martensitic transition in this series of $Ni_{2+x}Mn_{1-x}Ga$ compounds.

Martensitic transitions in $Ni_{2+x}Mn_{1-x}Ga$ were found to be first-order, as indicated by the hysteretic behavior in the electrical resistivity around the transition region. Recent experimental and theoretical studies have suggested the existence of 5-layer (in austenitic phase) and 7-layer (in martensite phase) phases and their conversion around 270 K.[2,6,12,35,36] Furthermore, the appearance of premartensitic transition in Ni_2MnGa seems to be very sample dependent. Some researchers have suggested that anomalous features between T_M and T_C is an indication of the occurrence of premartensitic transition in this class of materials, while others claimed that no sign of such transition can be resolved by various measurements.[2,7,15,28,37] Therefore, the underlying mechanisms leading to the above discussed phase transitions are not fully established.

In this paper, we report a systematic investigation of temperature-dependent transport and thermodynamic properties including electrical resistivity (ρ), specific heat (C_P), Seebeck coefficient (S), as well as thermal conductivity (κ) on $Ni_{2+x}Mn_{1-x}Ga$ with $0 \leqslant x \leqslant 0.24$. The present measurements were carried out by taking into consideration that these physical properties are expected to be very sensitive to the structural and magnetic transitions in this system.[2,3,20,35] Pronounced anomalous features and significant thermal hysteresis were observed in all measured physical properties near the structural (martensitic) phase transition. Particularly, there is an abrupt peak in κ near the martensitic transition, most likely due to the contributions from the soft phonons. In addition, the features of the premartensitic transition are studied in detail by means of these measurements. To the best of our knowledge, this study represents the first comprehensive report of transport and thermodynamic properties on the $Ni_{2+x}Mn_{1-x}Ga$ alloys.

II. EXPERIMENT

Polycrystalline $Ni_{2+x}Mn_{1-x}Ga$ samples with nominal compositions of $x=0$, 0.04, 0.06, 0.10, 0.14, 0.18, and 0.24 were prepared by conventional arc melting process in argon atmosphere. To promote homogeneity, the resulting ingots were annealed in a vacuum-sealed quartz tube at 800 °C for two days, followed by furnace cooling. For $x \leqslant 0.10$, the room-temperature x-ray spectra show the cubic $L2_1$ Heusler phase. On the other hand, the tetragonal phase was observed for $x > 0.10$ because the T_M's of these compositions are above room temperature. Resistivity measurements were carried out by standard four probe method in helium closed cycle refrigerator. Relative specific heats were performed with a high resolution ac calorimeter, using chopped light as a heat source. For appropriately chosen chopping frequency (typically 2–10 Hz), the magnitude of the temperature oscillation is inversely proportional to the total heat capacity (including sample and addendum). The thermal conductivity was carried out in a LHe/LN_2 cryostat from 10 to 400 K, using a direct heat-pulse technique. The sample was cut in to a rectangular parallelepiped shape with typical size of $1.5 \times 1.5 \times 5.0$ mm^3 with one end glued (with thermal epoxy) to a copper block that served as a heat sink, while a calibrated chip resistor as a heat source glued to the other end. The temperature difference was measured by an E-type differential thermocouple with junctions thermally attached to two well-separated positions along the longest axis of the sample. The temperature difference was controlled to be less than 1 K to minimize the heat loss through radiation. During measurements the sample space is maintained in a good vacuum (better than 10^{-4} Torr). For the Seebeck coefficient measurements, Seebeck voltages were detected using a pair of thin Cu wire electrically connected to the sample with sliver paint at the same positions as the junctions of differential thermocouple. The stray thermal emfs are eliminated by applying long current pulses ($\sim$100 s) to the chip resistor, where the pulses appear in an off-on-off sequence. All experiments were performed during warming with a rate slower than 20 K/h. The reproducibility of S and κ measurements is better than 2%, while the absolute accuracy of κ is approximately 15%, which mainly arises from the error in measuring the geometrical factor of the samples. The details of our measurement techniques can be found elsewhere.[38]

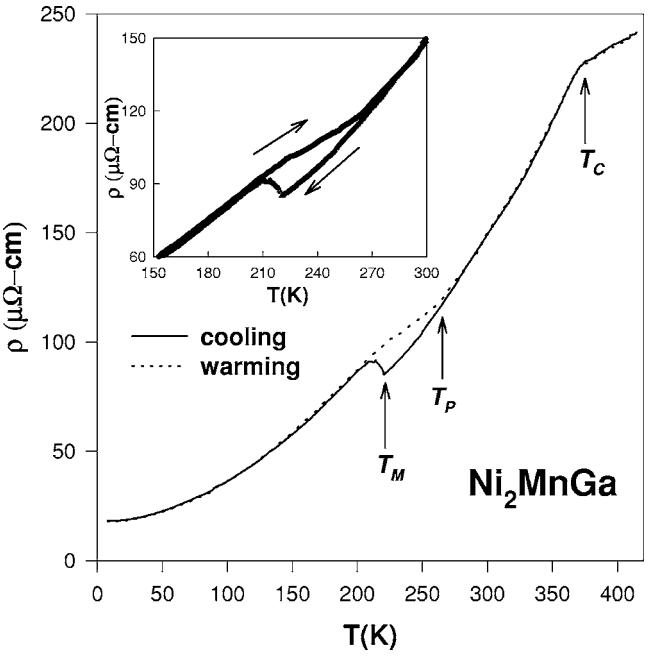

FIG. 1. Temperature dependence of the electrical resistivity of Ni_2MnGa measured on both cooling and heating. Inset: a close-up plot of the thermal hysteresis effect near the martensitic transition.

III. RESULTS AND DISCUSSIONS

A. Electrical resistivity

The temperature-dependent electrical resistivity $\rho(T)$ of the stoichiometric compound Ni_2MnGa is given in Fig. 1. The obvious slope change near 380 K is indicative of the ferromagnetic ordering. Below the Curie temperature (T_C), the resistivity shows a steep fall, which can be attributed to the disappearance of electrons scattering on magnetic fluctuations.[2,15,28,37] The behavior of ρ at Curie point is the

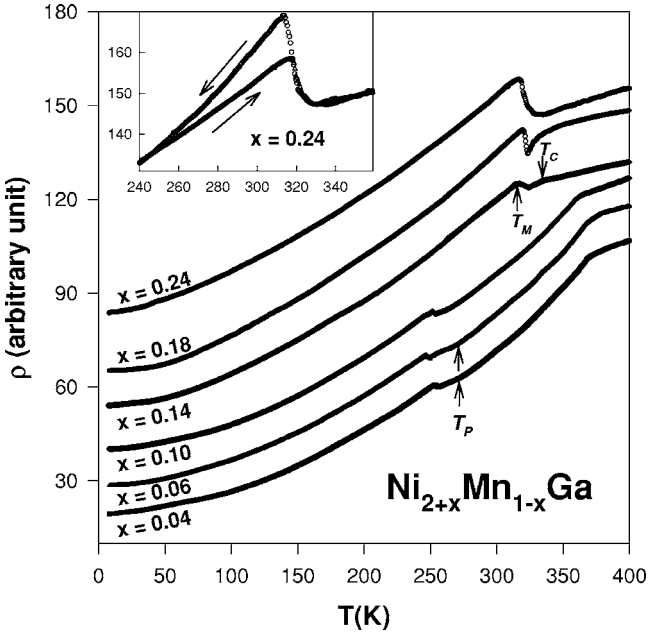

FIG. 2. Evolution of the temperature-dependent electrical resistivity in $Ni_{2+x}Mn_{1-x}Ga$ with $x=0.04-0.24$ on heating. Inset shows a blow-up plot near the phase transition for the $Ni_{2.24}Mn_{0.76}Ga$ compound.

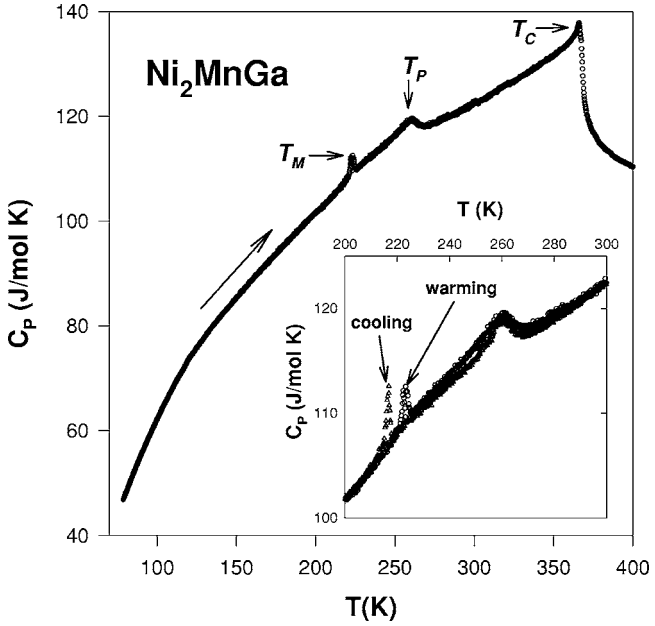

FIG. 3. Temperature variation of the observed specific heat in Ni_2MnGa. The inset illustrates an enlarged view near the martensitic and premartensitic transitions.

common feature for the Heusler compounds with magnetic ordering.[1] An apparent jumplike feature appears at around 220 K (T_M), signifying the occurrence of the martensitic transition. As the temperature lowers further, the electrical resistivity of Ni_2MnGa decreases, which represents a typical metallic behavior. A prominent thermal hysteresis loop was found between 210 K and 265 K, confirming the first-order nature of the structural (martensitic) phase transition. On the other hand, such a hysteretic feature is absent for the ferromagnetic transition, consistent with the results reported by others.[2,15,28,37] As seen in the inset of Fig. 1, a noticeable slope change in $\rho(T)$ around 265 K in the warming curve marks the finish of the martensitic transition (or the onset of the premartensitic transition), as evident by the merging of the warming and cooling $\rho(T)$ curves in this material.

Figure 2 shows the temperature-dependent electrical resistivity of $Ni_{2+x}Mn_{1-x}Ga$ with various values of x. All data shown in this figure were performed during warming process. Since the magnitude of ρ for these compounds are rather similar, we thus offset each $\rho(T)$ curve by 10 (arbitrary unit) for clarity. As seen from Fig. 2, distinct anomalous features in $\rho(T)$ at both T_C (a slope change) and T_M (a jump) can be resolved. Besides, it was generally found that as the value of x increases, T_C gradually decreases while T_M increases. For $x=0.14$, the martensitic and ferromagnetic transitions are found to be closing up on each other, and finally T_C and T_M coincide for the compositions with $x \geqslant 0.18$. Such a coincidence gives rise to a prominent peak in ρ around 320 K, signifying the coupling of structural and magnetic transitions, which is in well accordance with the other reported results.[2,15,20,28,37] A close-up ρ vs T plot near the phase transition for $Ni_{2.24}Mn_{0.76}Ga$ is illustrated in the inset of Fig. 2. As indicated in this figure, more pronounced anomalies in $\rho(T)$ around the martensitic transition with cooling process are generally observed in these materials.

Among the $Ni_{2+x}Mn_{1-x}Ga$ alloys we investigated, a change of slope in $\rho(T)$ near 260 K was observed for the compositions of $x=0.04$ and $x=0.06$ (indicated by the arrows in Fig. 2), suggesting the existence of the premartensitic transition in these compounds. However, no noticeable sign of premartensitic transition appear in the electrical resistivity data for larger x. The signature of this premartensitic transition in these compounds is more pronounced in the specific heat and thermal transport properties, which will be addressed in later sections. The previously reported results suggest that the 5M to 7M intermediate transitions increase the number of conduction electrons and hence the reduction in ρ would be expected.[2,6] A detailed analysis of various scattering mechanisms significant to the electrical resistivity has predicted that the electron-phonon scattering gives the dominant contribution in the whole temperature range for this class of materials, in comparison with the electron-magnon and vibrating impurities scattering. Further details can be seen elsewhere.[37]

B. Specific heat

The temperature-dependent specific heat (C_P) of Ni_2MnGa is illustrated in Fig. 3. Notice that the ac technique does not give the absolute value of specific heat without detailed knowledge of the power absorbed from the light pulse. The absolute value of the specific heat is obtained by normalizing our ac data to the previously reported result at 200 K.[4] The resulting temperature dependence and overall absolute values of specific heat are similar to those reported in Ref. 4. As demonstrated in Fig. 3, three distinct anomalies which correspond to the martensitic transition (at around

220 K), premartensitic transition (at around 260 K), and magnetic transition (at around 366 K) can be clearly identified by specific heat measurement. In the inset of Fig. 3, a close-up plot of C_P with heating and cooling cycles clearly reveals a thermal hysteretic behavior at the martensitic transition in Ni_2MnGa. However, no such kind of feature can be resolved at the premartensitic transition and magnetic transition. Since the specific heat measurement is known as a sensitive probe of phase transitions involving entropy change, the existence of premartensitic transition in the shape memory alloy Ni_2MnGa is unambiguously detected by our high resolution ac calorimeter. The excess specific heat $\Delta C_p/C_p$ was estimated to be about 4% (heating cycle) and 3% at T_M and T_P, respectively. As the premartensitic transition is the tip-off of the beginning of martensitic transition, it is reasonable to notice that the premartensitic transition found in this material shows a wider transition width and smaller excess specific heat than that of the martensitic transition itself.

At T_C, it is found that the specific heat exhibits pronounced peak during the magnetic phase transition due to a large amount of entropy associated with the paramagnetic to ferromagnetic ordering. The entropy change ΔS associated with each phase transition in the present case is difficult to estimate precisely because these phase transitions overlap and the lattice background is hard to define. We have noticed that the excess specific heat $\Delta C_p/C_p$ ($\sim 4\%$) at T_M observed by our ac technique is smaller than that reported by Kreissl *et al.* (adiabatic technique).[4] This discrepancy is not likely due to the sample quality, since the transition width, determined from the temperature width of half maximum, of about 3 K in our present study is narrower than that presented by Kreissl and co-workers. Even though the ac technique has the advantages of great precision and only a small sample needed, the latent heat usually accompanying with a first-order phase transition is difficult to measure. Therefore, there might be some contribution from latent heat during the martensitic transition which is missing by our specific heat measurement. However, the transition temperatures, characteristics for the premartensitic transition and magnetic transition determined from our ac specific heat measurements are still valid.

The T-dependent specific heat of the compositions $x=0.04$, 0.06, 0.10, 0.14, 0.18, and 0.24 taken with warming process are shown in Fig. 4. Each curve is offset by 20 (J/mol K) for clarity. Two kinds of distinct features can be seen form C_P measurements. For $x \leqslant 0.10$, two phase transitions at T_M (around 260 K) and T_C (around 360 K) are clearly visible in these compounds. As a function of Ni concentration, T_C gradually decreases and overlaps with the martensitic transition around 310 K. For $x \geqslant 0.14$, only one pronounced peak (around 310 K) in C_P is found and it is highly hysteretic (see the inset of Fig. 4). For the $x=0.14$ sample, there is a noticeable shoulder right below the peak position, suggesting the martensitic transition and magnetic transition have not yet completely merged at this composition, consistent with the result of electrical resistivity measurement.

A remarkable feature is the observation of premartensitic transition around 260 K for the compositions $x \leqslant 0.06$,

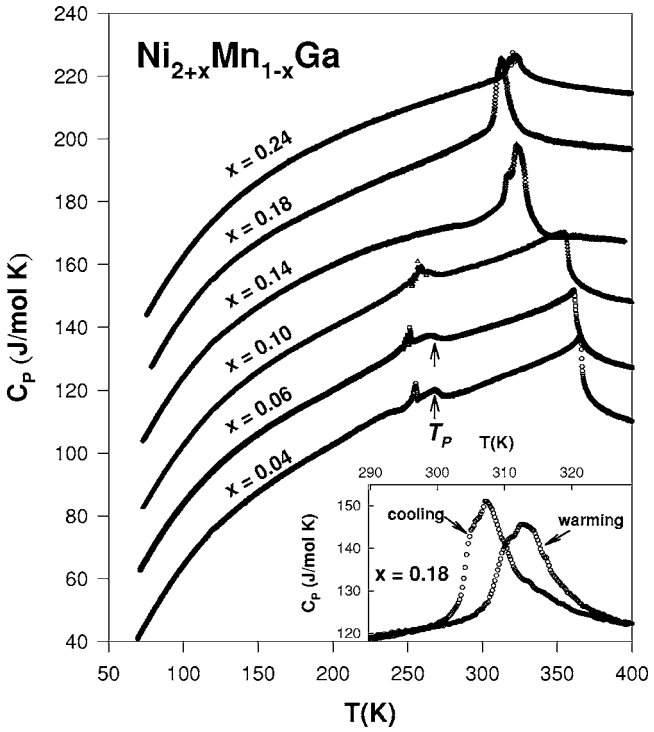

FIG. 4. The temperature dependent specific heat for $Ni_{2+x}Mn_{1-x}Ga$ with $x=0.04-0.24$ on heating. Each curve is offset by 20 J/mol K for clarity. The inset shows the thermal hysteretic behavior in C_P near the phase transition for the $x=0.18$ compound.

as indicated by the arrows in Fig. 4. The temperature (~ 260 K) at which the premartensitic transition occurs is almost composition-independent, and completely disappears for the compositions $x \geqslant 0.10$. This is in good agreement with the previously reported results.[2,22] Another interesting aspect is that the anomalies at T_M contain many small satellite peaks (or scatters). Such a feature is more apparent in the $x=0.10$ sample (see Fig. 4). These satellite peaks indicate that the structural transition takes place in multiple steps. This is also consistent with the previously reported DSC measurements.[39] Due to the absence of configuration contributions to the entropy in the case of martensitic transformations, it is assumed that the total entropy has three main contributions, namely, electronic, magnetic, and vibrational.[12] Previous reports have indicated that the electronic contribution is very small and the vibrational contribution is independent of composition.[12,40] This leads to the conclusion that the increase in entropy for Ni excess alloys is mainly due to the magnetic contribution. This is further supported by the strong increase in the magnetization jump for the Ni excess alloys.[41] In this regard, the observed peaks in specific heat measurements are more pronounced for Ni excess alloys.

C. Seebeck coefficient

The temperature-dependent Seebeck coefficient $S(T)$ with warming process for Ni_2MnGa ($x=0$) is displayed in Fig. 5. The Seebeck coefficient of Ni_2MnGa is negative for the entire temperature range under investigation, regardless of the

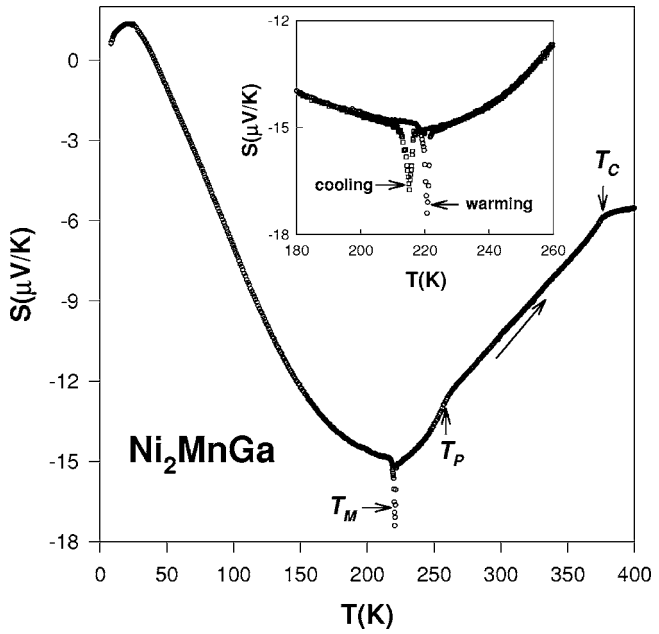

FIG. 5. Seebeck coefficient vs temperature in Ni_2MnGa on heating. Inset: a close-up plot near T_M with both cooling and heating runs.

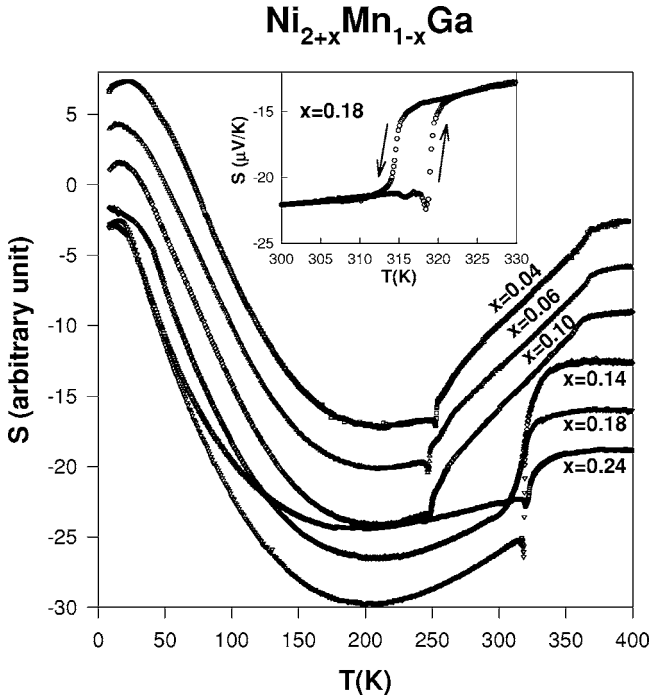

FIG. 6. Evolution of the temperature-dependent Seebeck coefficient in $Ni_{2+x}Mn_{1-x}Ga$ with $x=0.04-0.24$ on heating. Inset shows the blowup plot near the phase transition for $Ni_{2.18}Mn_{0.82}Ga$ compound.

positive phonon-drag effect at low temperature. The negative S value for this compound suggests that electron-type carriers dominate the thermoelectric transport. With decreasing temperature, a clear change of slope to a larger dS/dT value was found near T_C, similar to that of the electrical resistivity data. In the vicinity of T_M, the Seebeck coefficient exhibits a pronounced peak with $\Delta S/S \sim 20\%$ within a narrow temperature interval of about 5 K. Notice that an apparent thermal hysteresis loop was also observed near T_M, as displayed in the inset of Fig. 5. In addition, a distinct kink around $T_P \sim 260$ K (indicated by arrows in Fig. 5) signifies the occurrence of the premartensitic transition, in agreement with the specific measurement. Theoretical and experimental studies have suggested that significant changes take place at the Fermi surface associated with the phase transitions in Ni_2MnGa.[2,35,42,43] Since the Seebeck coefficient measurement is a sensitive probe of energy relative to the Fermi surface, the result of Seebeck coefficient measurement would provide valuable information toward the understanding of the influences to the band structure in Ni_2MnGa during these phase transitions.[37,44,45] The steep fall of Seebeck coefficient near the ferromagnetic transition is ascribed to a reduction of magnetic scattering to the thermoelectric transport at T_C. Such an anomalous feature is consistent with the band structure calculations, which suggest that the density of states (DOS) at the Fermi surface reduces significantly due to ferromagnetic ordering.[35] On the other hand, the prominent anomalous peak in S suggests a strong modification of band structure at T_M, associated with the structural change near the phase transition. For ordinary metals, Seebeck coefficient is often discussed using the well-known Mott formula (electronic contribution),

$$S_e \propto \frac{1}{e}\left(\frac{1}{N(E)}\frac{\partial N(E)}{\partial E}\right)_{E=E_F}, \quad (1)$$

assuming a one-band model with an energy-independent relaxation time, where e is the elementary charge, and $N(E)$ is the electronic DOS. Equation (1) indicates that any change in the Seebeck coefficient is a direct consequence of the modifications in the DOS near the Fermi level.[43,46] Another peculiar feature of the Seebeck coefficient in Ni_2MnGa is the appearance of a broad minimum at around 220 K (happen to be close to T_M), indicating the existence of a pseudogap in the electronic density of states in this material. Such a pseudogap feature is well-documented for other Heusler compounds.[47,48]

In Fig. 6, we display the temperature-dependent Seebeck coefficient of $Ni_{2+x}Mn_{1-x}Ga$ with various x values, measured in the warming process. Again, each curve is offset for clarity. The room temperature S found to be negative, revealing that the majority charge carriers are electrons irrespective of their compositions. The composition dependent Seebeck coefficient shows three different trends as a function of temperature. First, the $S(T)$ behavior is nearly identical for the low Ni substituted samples with $x=0.04$, 0.06, and 0.10. A small but detectable variation in the slope of S around 260 K for $x=0.04$ and 0.06, similar to that of the stoichiometric compound ($x=0$), indicates the premartensitic transition. The observed premartensitic transitions are attributed to a small tetragonal distortion, whereas the martensitic transition is associated with considerably larger tetragonal distortion. However, such a signature of premartensitic transition is invisible

for $x \geqslant 0.10$, which is in good agreement with our specific heat results and previous findings.[2,28] This can be attributed to the assessment that the increase in conduction electron upon Ni substitution to the level up to which the premartensitic transition can take place by not significantly altering the particular part of the multiply connected Fermi surface.[2] Second, for $x=0.14$, the Seebeck coefficient decreases with increasing temperature and then develops a broad minimum at around 220 K. With further increasing temperature a significant jump in S around 310 K to 330 K was found, presumably due to T_M and T_C approaching each other or T_M and T_C separated by a close interval of temperature. Finally, for the excess Ni substituted samples with $x=0.18$ and 0.24, $S(T)$ shows an abrupt jump associated with a well-defined spike near 320 K as the T_M and T_C couples. The phase transition was again found to be strongly hysteretic, as shown in the inset of Fig. 6. Such a distinctive jump in S is remarkable in the sense that no similar feature has been observed in the electrical transport.

Another systematic variation with respect to Ni content is that the broad minima in S shift to lower temperature with larger x value ($\sim$200 K for $x=0.18$ and $\sim$170 K for $x=0.24$). The upturn in S at high temperatures is presumably attributed to the contribution of thermally excited quasiparticles across their pseudogaps. As the temperature increases, intrinsic electrons and holes are excited. If the holes have a slightly higher mobility than the electrons in these materials, the thermal transport is increasingly governed by p-type carriers and the negative Seebeck coefficient reduces after passing the broad maximum. If the rigid-band shift of E_F from near the valley of pseudogap to a slightly above the center with increasing x value, then it would require lower activated energy for quasiparticles thermally excited across the pseudogap. Such an interpretation can qualitatively explain the tendency that the minimum position in S shifts to lower temperatures with increasing Ni substitution.

Now we discuss the anomalous feature near the martensitic transition for $Ni_{2+x}Mn_{1-x}Ga$. In comparison with the electrical resistivity data, these abrupt jumps and spike-shape features are unique and significant, representing sensitive nature of S towards the martensitic transition in this series of alloys. It is worth mentioning that our S data for Ni_2MnGa has a very similar temperature variation to that of the nonmagnetic shape memory alloy NiTi,[44,49] except for the opposite sign. This can be correlated with the predictions made from theoretical investigations of Ni(Ti/Al) and Ni_2MnGa, as these two systems have rather similar Fermi surface.[8,11,22,23,35,50,51] Therefore, the anomalous feature in S is mainly arising from the change of the Fermi surface as the material undergoes the martensitic transition. However, the spike-shape peak in S is very unusual. This could be connected to the scattering with the heat carrying soft phonons, which will be described in the following section. During cubic to tetragonal structural transition, changes in the lattice as well as electronic levels take place. Further the splitting causes the redistribution electrons, which in turn drives the structural transition described by the band Jahn-Teller effect. These appreciable changes are expected to exhibit the corresponding predominant changes in the observed Seebeck coefficient in these $Ni_{2+x}Mn_{1-x}Ga$ alloys. Unfortunately, there were no substantial reports of Seebeck coefficient measurement available in this type of compound except the one recently published by Priolker *et al.*[45] However, the anomalous S features reported by the authors were not as pronounced as the present observations, presumably due to sample quality and/or measurement technique.

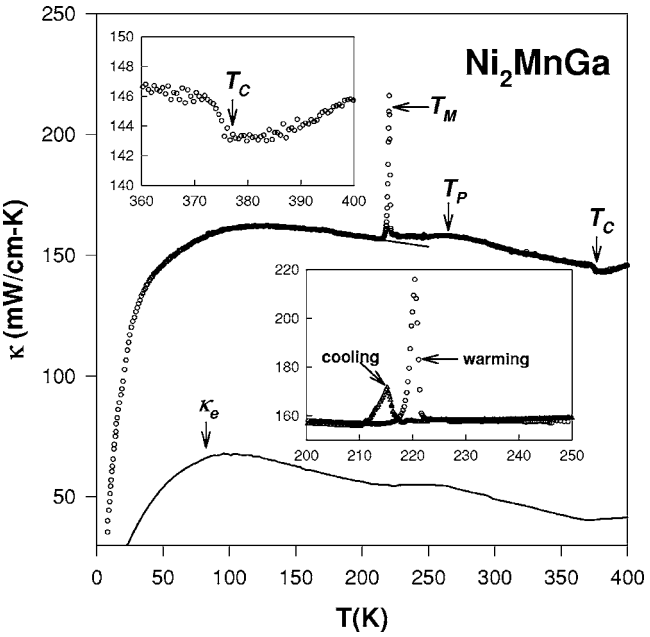

FIG. 7. Thermal conductivity as a function of temperature for Ni_2MnGa on heating. Estimated electronic (κ_e) contribution to the total thermal conductivity is given as a solid line. Inset: a blow-up plot for the observed thermal conductivity near the magnetic transition (upper) and martensitic transition (lower).

D. Thermal conductivity

The temperature-dependent thermal conductivity $\kappa(T)$ with warming process for the stoichiometric Ni_2MnGa is shown in Fig. 7. The magnitude of room-temperature thermal conductivity is approximately 150 mW/K cm. With raising temperature, κ increases until a broad maximum occurring at around 100 K, which is due to the reduction of thermal scattering at low temperatures. The maximum takes place at the temperature where the phonon mean free path is approximately equal to the crystal site distance. Around the martensitic transition temperature $T_M \sim 220$ K, κ exhibits a steplike jump accompanied by a remarkable spike-shaped peak with $\Delta\kappa/\kappa \sim 40\%$. As temperature increases further, a notable slope change at $T_P \sim 260$ K signifies the existence of the premartensitic transition in this compound, consistent with the specific heat and Seebeck coefficient results. Above T_P, κ drops with increasing temperature, following the approximately $1/T$ behavior. Such a temperature variation is commonly seen at high temperatures for crystallized solids. Near the Curie temperature ($T_C \sim 380$ K), κ shows a noticeable drop (see the upper inset of Fig. 7) presumably due to an increase of magnetic scattering in the paramagnetic state. In addition, significant thermal hysteresis between heating and cooling was also observed near the martensitic transition, as

shown in the lower inset of Fig. 7. Similar to that of the specific heat and Seebeck coefficient data, the cooling run has a less pronounced anomaly than that of the warming run. Since the thermal conductivity measurements provide valuable information about the various scattering processes of thermal carriers, the present data would offer an opportunity to probe the interplay between the lattice, charge, and magnetic degrees of freedom in these shape memory alloys.

In general, the total thermal conductivity for a metal can be expressed as a sum of lattice κ_L and electronic κ_e terms: $\kappa=\kappa_L+\kappa_e$. The electronic contribution is estimated by means of the Wiedemann-Franz Law: $\kappa_e\rho/T=L_0$. Here ρ is the dc electrical resistivity and $L_0=2.45\times10^{-8}$ W Ω K^{-2} is the Lorentz number. We thus calculate κ_e using the Wiedemann-Franz Law and the measured ρ data. As illustrated in Fig. 7, the solid lines represent calculated κ_e for Ni_2MnGa, and the electrical thermal conductivity κ_e is found to be about one-third of total thermal conductivity. From this estimation, it is clearly seen that the anomalous features in κ at T_P and T_C are essentially electronic origin. However, the significant spike-shaped peak in the vicinity of the martensitic transition cannot be explained by the electronic contribution, but must be due to the change of lattice thermal conductivity κ_L during the transition.

By the generalized simple equation, the lattice thermal conductivity is given as $\kappa_L=C_v v l$,[52] where C_v is the phonon specific heat, v represents the phonon drift velocity, and l is the mean free path. The phonon drift velocity and mean free path are expected not to be greatly influenced by the transition. However, a pronounced specific heat peak with $\Delta C_P/C_P\sim40\%$ was reported by Kreissl *et al.* for Ni_2MnGa, which well accounts for the observed peak in κ[4]. Note that similar peak features in κ were also seen in the charge-density-wave (CDW) materials, which undergoes the Peierls transition at low temperatures.[53–56] The appearance of Kohn anomaly and the anomalous heat carried by the soft phonons were suggested as possible origins for such peaks in thermal conductivity.[38,53,55] The martensitic transition and the Peierls transition exhibit striking similarities, such as the existence of the soft phonon modes. Recent theoretical studies also indicated that the structural transition in Ni_2MnGa is very similar to that of the Peierls transition.[35] Inelastic neutron scattering studies have revealed a significant $[\zeta\ \zeta\ 0]$ TA_2 phonon softening near T_M with a wave vector $\zeta_0=0.33$ in Ni_2MnGa. Besides, A-15 compounds with similar structural transition and α-U are also the well-known examples with Jahn-Teller distortion involved.[57–59] A comprehensive theoretical approach to relate the two types of transitions could be seen in the theoretical work carried out by Bhatt *et al.*[57,60]

A detailed analysis of specific heat in the Peierls transition region indicated that the coherence length ξ_0 must be short enough for a significant contribution from the lattice.[53,56] We have recently reported that the coherence length ξ_0 of the strong-coupled CDW systems $R_5T_4Si_{10}$ (R=rare-earth elements; T=Ir,Rh) is as short as 5 Å.[61] Consequently, there are a large number of soft phonon modes in the transition region which provides a substantial specific heat arising from their occupation. Since the softening modes near $2k_F$ are propagating, the heat carried by the soft phonons is considerable and is most likely responsible for the giant thermal conductivity peak. Hence, both specific heat and thermal conductivity features around the Peierls transition could be qualitatively understood in terms of this picture. This scenario is also applicable in the present case, where Ni_2MnGa has been found to possess short coherence length.[62] Therefore, the giant thermal conductivity peak appeared in Ni_2MnGa near T_M can be qualitatively understood with the appearance of additional heat carrying soft phonons.

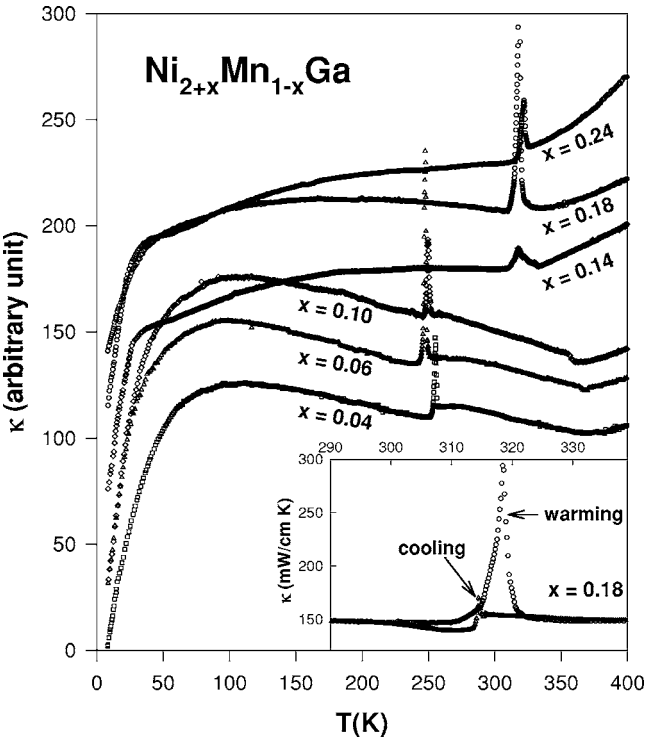

FIG. 8. Evolution of the temperature-dependent thermal conductivity in $Ni_{2+x}Mn_{1-x}Ga$ with $x=0.04-0.24$ on heating. Inset shows the blowup plot near the phase transition for $Ni_{2.18}Mn_{0.82}Ga$.

Figure 8 illustrates the temperature-dependent thermal conductivity of $Ni_{2+x}Mn_{1-x}Ga$ alloys with various values of x. Note that each curve is offset and taken with warming process. The value of room-temperature thermal conductivity for all compositions is found to be nearly equal with a magnitude of approximately 150 mW/K cm. The small variation of κ(RT) in these alloys is within the uncertainty of our measurement technique. As seen from Fig. 8, the composition dependent on thermal conductivity shows two distinct temperature variations. The low Ni substituted samples with $x=0.04$, 0.06, and 0.10 show rather similar $\kappa(T)$ to that of the stoichiometric Ni_2MnGa sample, except the variation near the transition temperatures. The slope change in κ at T_P is still visible for the $x=0.04$ and 0.06 samples, in accordance with the specific heat and Seebeck coefficient data. As the Ni content increases ($x=0.10$, 0.18, and 0.24), the broad maximum at low temperatures evolves into a plateau toward higher temperatures, and T_C and T_M coincides at around 320 K for the composition $x=0.18$. The disappearance of the low-temperature maximum in κ is presumably due to the enhanced phonon scattering from point defects in the heavily substituted samples. In the case of composition with $x=0.14$, T_C and T_M are closing up, and $\Delta\kappa$ is found to be

considerably smaller than all other compositions. This is most likely that two approaching phase transitions with very different origins in nature interfere with each other, resulting in a mixed transport response in this material. For $x \geqslant 0.18$, a single peak appears near 320 K as a result of coupling of T_M and T_C, which is in good agreement with previously reported results.[2,12,15,28] It is worthwhile mentioning that a huge thermal conductivity peak ($\Delta\kappa/\kappa \sim 100\%$) near T_M within a narrow temperature range of 10 K was observed for $x=0.18$ (see the lower inset of Fig. 8). Such a tremendous phenomenon among the thermal transport properties, to the best of our knowledge, is unique to the martensitic transition in the shape memory alloys and definitely warrants further investigations.

E. Compositional dependence on transition temperatures

From the above transport and thermodynamic measurements, two groups of samples, above and below $x=0.14$ (or with T_M above and below 270 K), with distinct physical properties were observed. Existence of such different groups based on the composition or T_M has already been reported.[12] It has been suggested that the alloys with high T_M (above 270 K) are expected to have seven-layered martensitic structure, where as the alloys with low T_M (below 270 K) undergo structural transformation to the five-layered martensitic structure.[2,12] The existence of premartensitic transition is found in the low Ni concentration samples ($x \leqslant 0.06$), and the temperature at which this transition occurs is rather independent of the composition ($T_P \sim 260$ K). For the $x=0.10$ sample, the premartensitic transition diminishes by overlapping with martensitic transition at around 270 K, consistent with the previous report that premartensitic transition appears only for the sample with $T_M < \sim 270$ K.[2,28] For the $x=0.14$ sample, the martensitic and magnetic phase transitions were found to be overlapping, and the transition temperature takes a sudden jump to around 310 K. For samples with $x \geqslant 0.18$, T_M and T_C completely couple to each other, as evidenced by the single anomaly in all measured properties. However, in each of these two groups, T_M and T_C do not vary significantly until a sudden jump of transition temperature occurs at a critical composition $x_C=0.14$. We speculate that the five-layered and seven-layered modulations play an important role in the determination of the structural transition temperature. For a particular composition, martensitic transition temperature may differ significantly depending on the modulation phases. The alloys with five-layered (seven-layered) modulation undergo a martensitic transition at a lower (higher) temperature. The substitution of Ni in place of Mn decreases the amount of five-layered modulation but enhances the seven-layered modulation. A sudden jump of T_M at the critical composition $x_C=0.14$ would correspond to a complete transformation from five-layered to seven-layered modulation in this compound. Such behavior has been also observed by others.[12]

Further, we notice that the variation of T_M as a function of Ni concentration is not as systematic as T_C, which lead to the speculation that T_M may be slightly sample dependent. A recent report also indicated that the martensitic transition temperatures differ slightly for different samples of the same composition.[12] This is further evident from the different values of T_M given in the literature, presumably due to the structural disorder and/or deviations from the nominal composition.[41] Nevertheless, it was found that both T_M and T_C appear at nearly identical temperatures in different measured physical properties for a particular composition, and the overall variation of T_M shows an increasing tendency as a function of Ni concentration. Therefore we believe that the observed anomalous features in the thermodynamic and transport properties are intrinsic to the alloys investigated.

F. Thermal hysteresis

Lastly we discuss another interesting feature exhibited in these alloys, namely the thermal hysteretic behavior in the vicinity of the martensitic transition. From Fig. 1 to Fig. 8, we have presented the significant difference in all measured transport and thermodynamic properties between cooling and heating runs in these selected compositions. Actually, such hysteretic behavior at T_M exists in all compositions we investigated. This effect was also found in the well-known shape memory compound NiTi, and the reported Seebeck coefficient in NiTi is very similar to our results.[44,49] Another notable feature is the reduction in the height of the peak during the cooling process in S and κ, and the T_M determined from the cooling run is always several degrees lower than that of the warming run. On the other hand, the electrical resistivity data show an opposite hysteretic behavior to the thermal transport measurements, as the cooling run shows a more pronounced anomaly at T_M. Therefore, for a given thermal cycle (cooling and heating), the thermal properties (C_P, S, as well as κ) exhibit rather different hysteretic behavior than that of the electrical transport property (ρ). Such a hystereses effect is presumably due to the presence different modulated structures of 5M and 7M.[6] It has been suggested that these modulated structures have different type of Fermi surface nesting, thus also the conduction electron density.[35,6] During heating the 7M to 5M reverse transition is absent,[6] leading to the observed difference in these transport properties during thermal cycles.

IV. CONCLUSION

In summary, we have performed a systematic investigation of temperature-dependent transport and thermodynamic properties including electrical resistivity (ρ), specific heat (C_P), Seebeck coefficient (S), and thermal conductivity (κ) on the $Ni_{2+x}Mn_{1-x}Ga$ Heusler compounds with $0 \leqslant x \leqslant 0.24$. Two groups of samples, above and below $x=0.10$ (or with T_M above and below 270 K), exhibit distinct behavior in the presented physical properties. Pronounced anomalous features and significant thermal hysteresis were observed in all measured quantities near the martensitic phase transitions. In particular, there is an abrupt peak in κ near the martensitic transition, presumably due to the contribution from the soft phonons. Existence of premartensitic transition was unambiguously resolved in the low Ni concentration samples, and becomes less distinctive with larger x. Our present study

constitutes the most thorough transport and thermodynamic measurements on the shape memory alloy Ni_2MnGa and the effects of Ni excess to the parent compound. However, the observed giant thermal conductivity peak near the martensitic phase transition in these alloys is quite unusual and warrants further investigations.

ACKNOWLEDGMENTS

This work was supported by the National Science Council, Taiwan, under Grants Nos. NSC-93-2112-M-259-004 (Y.K.K.) and NSC-93-2112-M-006-001 (C.S.L.).

[1] A. Hamzic, R. Asomoza, and I. A. Campbell, J. Phys. F: Met. Phys. **11**, 1441 (1981).
[2] V. V. Khovailo, V. Takagi, A. D. Bozhko, M. Matsumoto, J. Tani, and V. G. Shavrov, J. Phys.: Condens. Matter **13**, 9655 (2001).
[3] P. J. Brown, J. Crangle, T. Kanomata, M. Matsumoto, K.-U. Neumann, B. Ouladdiaf, and K. R. A. Ziebeck, J. Phys.: Condens. Matter **14**, 10159 (2002).
[4] M. Kreissl, K.-U. Neumann, T. Stephens, and K. R. A. Ziebeck, J. Phys.: Condens. Matter **15**, 3831 (2003).
[5] P. J. Brown, B. Dennis, J. Crangle, T. Kanomata, M. Matsumoto, K.-U. Neumann, L. M. Justham, and K. R. A. Ziebeck, J. Phys.: Condens. Matter **16**, 65 (2004).
[6] V. V. Khovailo, K. Oikawa, C. Wedel, T. Takagi, T. Abe, and K. Sugiyama, J. Phys.: Condens. Matter **16**, 1951 (2004).
[7] F. Zuo, X. Su, P. Zhang, G. C. Alexandrakis, F. Yang, and K. H. Wu, J. Phys.: Condens. Matter **11**, 2821 (1999).
[8] A. Zheludev, S. M. Shapiro, P. Wochner, A. Schwartz, M. Wall, and L. E. Tanner, Phys. Rev. B **51**, 11310 (1995).
[9] A. Ayuela, J. Enkovaara, and R. M. Nieminen, J. Phys.: Condens. Matter **14**, 5325 (2002).
[10] A. Ayuela, J. Enkovaara, K. Ullakko, and R. M. Nieminen, J. Phys.: Condens. Matter **11**, 2017 (1999).
[11] L. Manosa, A. Planes, J. Zarestky, T. Lograsso, D. L. Schlagel, and C. Stassis, Phys. Rev. B **64**, 024305 (2001).
[12] V. V. Khovailo, K. Oikawa, T. Abe, and T. Takagi, J. Appl. Phys. **93**, 8483 (2003).
[13] A. Fujita, K. Fukamichi, F. Gejima, R. Kainuma, and K. Ishida, Appl. Phys. Lett. **77**, 3054 (2000).
[14] A. T. Zayak and P. Entel, Mater. Sci. Eng., A **378**, 419 (2004).
[15] A. N. Vasil'ev, A. D. Bozhko, V. V. Khovailo, I. E. Dikshtein, V. G. Shavrov, V. D. Buchelnikov, M. Matsumoto, S. Suzuki, T. Takagi, and J. Tani, Phys. Rev. B **59**, 1113 (1999).
[16] P. J. Brown, A. Y. Bargawi, J. Crangle, K.-U. Neumann, and K. R. A. Ziebeck, J. Phys.: Condens. Matter **11**, 4715 (1999).
[17] N. Lanska, O. Soderberg, A. Sozinov, Y. Ge, K. Ullakko, and V. K. Lindroos, J. Appl. Phys. **95**, 8074 (2004).
[18] O. Heczko and L. Straka, J. Magn. Magn. Mater. **272–276**, 2045 (2004).
[19] G. Fritsch, V. V. Kokorin, and A. Kempf, J. Phys.: Condens. Matter **6**, L107 (1994).
[20] V. V. Khovailo, T. Takagi, J. Tani, R. Z. Levitin, A. A. Cherechukin, M. Matsumoto, and R. Note, Phys. Rev. B **65**, 092410 (2002).
[21] L. Manosa, A. Gonzalez-Comas, E. Obrado, A. Planes, V. A. Chernenko, V. V. Kokorin, and E. Cesari, Phys. Rev. B **55**, 11068 (1997).
[22] T. E. Stenger and J. Trivisonno, Phys. Rev. B **57**, 2735 (1998).
[23] A. Zheludev, S. M. Shapiro, P. Wochner, and L. E. Tanner, Phys. Rev. B **54**, 15045 (1996).
[24] P. A. Lindgard and O. G. Mouritsen, Phys. Rev. B **41**, 688 (1990).
[25] Claudia Bungaro, K. M. Rabe, and A. Dal Corso, Phys. Rev. B **68**, 134104 (2003).
[26] V. V. Kokorin, V. A. Chernenko, J. Pons, C. Segu, and E. Cesari, Solid State Commun. **101**, 7 (1997).
[27] U. Stuhr, P. Vorderwisch, V. V. Kokorin, and P. A. Lindgard, Phys. Rev. B **56**, 14360 (1997).
[28] V. D. Buchel'nikov, A. T. Zayak, A. N. Vasil'ev, D. L. Dalidovich, V. G. Shavrov, T. Takagi, and V. V. Khovailo, J. Exp. Theor. Phys. **92**, 1010 (2001).
[29] A. Gonzalez-Comas, E. Obrado, L. Manosa, A. Planes, V. A. Chernenko, B. J. Hattink, and A. Labarta, Phys. Rev. B **60**, 7085 (1999).
[30] E. Vives and A. Planes, Phys. Rev. B **50**, 3839 (1994).
[31] F. J. Perez-Reche, M. Stipcich, E. Vives, L. Manosa, A. Planes, and M. Morin, Phys. Rev. B **69**, 064101 (2004).
[32] F. J. Perez-Reche, E. Vives, L. Manosa, and A. Planes, Phys. Rev. Lett. **87**, 195701 (2001).
[33] A. Planes, F. J. Perez-Reche, E. Vives, and L. Manosa, Scr. Mater. **50**, 181 (2004).
[34] F. J. Perez-Reche, E. Vives, L. Manosa, and A. Planes, Mater. Sci. Eng., A **378**, 353 (2004).
[35] O. I. Velikokhatnyi and I. I. Naumov, Phys. Solid State **41**, 617 (1999).
[36] J. Enkovaara, A. Ayuela, A. T. Zayak, P. Entel, L. Nordstorm, M. Dube, J. Jalkanen, and R. M. Nieminen, Mater. Sci. Eng., A **378**, 52 (2004).
[37] Y. Zhou, Xuesong Jin, Huibin Xu, Y. V. Kurdryavtsev, Y. P. Lee, and J. Y. Lee, J. Appl. Phys. **91**, 9894 (2002).
[38] Y. K. Kuo, C. S. Lue, F. H. Hsu, H. H. Li, and H. D. Yang, Phys. Rev. B **64**, 125124 (2001).
[39] F. Q. Zhu, F. Y. Yang, C. L. Chien, L. Ritchie, G. Xiao, and G. H. Wu, J. Magn. Magn. Mater. **288**, 79 (2005).
[40] M. Matsumoto, M. Ebisuya, T. Kanomata, R. Note, H. Yoshida, and T. Kaneko, J. Magn. Magn. Mater. **239**, 521 (2002).
[41] V. V. Khovailo, V. Novosad, T. Takagi, D. A. Filippov, R. Z. Levitin, and A. N. Vasil'ev, Phys. Rev. B **70**, 174413 (2004).
[42] C. Jiang, G. Feng, S. Gong, and H. Xu, Mater. Sci. Eng., A **342**, 231 (2003).
[43] S. Fujii, S. Ishida, and S. Asano, J. Phys. Soc. Jpn. **58**, 3657 (1989).
[44] I. Yoshida, T. Ono, K. Iino, and D. Monma, IEEE, 20th International Conference on Thermoelectrics (2001), p. 495.
[45] K. R. Priolkar, P. A. Bhobe, S. D. Sapeco, and R. Paudel, Phys. Rev. B **70**, 132408 (2004).
[46] C. S. Garde and J. Ray, J. Phys.: Condens. Matter **14**, 3775 (2002).
[47] Yoshi Nishino, Intermetallics **8**, 1233 (2000).

[48] I. Galanakis, P. H. Dederichs, and N. Papanikolaou, Phys. Rev. B **66**, 134428 (2002).
[49] J. Y. Lee, G. C. Mcintosh, A. B. Kaiser, and Y. W. Park, J. Appl. Phys. **89**, 6223 (2001).
[50] Y. Lee, J. Y. Rhee, and B. N. Harmon, Phys. Rev. B **66**, 054424 (2002).
[51] M. Stipcich, L. Manosa, A. Planes, M. Morin, J. Zarestky, T. Lograsso, and C. Stassis, Phys. Rev. B **70**, 054115 (2004).
[52] Jerzy Bodzenta, Chaos, Solitons Fractals **10**, 2087 (1999).
[53] R. S. Kwok and S. E. Brown, Phys. Rev. Lett. **63**, 895 (1989).
[54] A. Smontara, K. Biljakovic, and S. N. Artemenko, Phys. Rev. B **48**, 4329 (1993).
[55] C. S. Lue, Y. K. Kuo, F. H. Hsu, H. H. Li, H. D. Yang, P. S. Fodor, and L. E. Wenger, Phys. Rev. B **66**, 033101 (2002).
[56] R. S. Kwok, G. Gruner, and S. E. Brown, Phys. Rev. Lett. **65**, 365 (1990).
[57] R. N. Bhatt and W. L. Mcmillan, Phys. Rev. B **14**, 1007 (1976).
[58] T. Castan, A. Planes, and A. Saxena, Phys. Rev. B **67**, 134113 (2003).
[59] C. H. Chen and G. H. Lander, Phys. Rev. Lett. **57**, 110 (1986).
[60] R. N. Bhatt, Phys. Rev. B **17**, 2947 (1978).
[61] Y. K. Kuo, F. H. Hsu, H. H. Li, H. F. Huang, C. W. Huang, C. S. Lue, and H. D. Yang, Phys. Rev. B **67**, 195101 (2003).
[62] U. Stuhr, P. Vorderwisch, and V. V. Kokorin, Physica B **234–236**, 135 (1997).